Drag On Ellipsoids at Finite Reynolds Numbers

B. J. O'Donnell and B. T. Helenbrook
Department of Mechanical and Aeronautical Engineering
Clarkson University, Potsdam, NY 13699

Numerical results for two-dimensional axisymmetric flow of an incompressible fluid over ellipsoidal particles are presented for Reynolds numbers from 0.1 to 200. A *hp*-finite element method is employed to obtain values of drag around particles ranging from spheres to discs. The results are compared to previous numerical, analytical, and experimental work presented in the literature. Using this data, a new drag model is created that predicts the drag on oblate ellipsoids ranging from spheres to discs. The new model is accurate to within 1.5% over the desired range of parameters.

1. **Introduction**

Lagrangian-Eulerian spray simulations require a drag model to predict the evolution of the droplets. Since liquid drops are typically more viscous than the surrounding gas, the drag is often modeled by that of a solid sphere. However depending on the flow conditions, drops can become significantly deformed and thus, it is important to incorporate the effect of the shape of the drop. Several models incorporating this effect have been proposed, but none have been rigorously tested at finite Reynolds numbers.

Happel and Brenner [1] and Clift et al. [2] provide theoretical solutions to low Reynolds number flows over non-spherical particles. While their results are accurate in Stokes flow, there are significant deviations at higher Reynolds numbers. For discs, experimental [3] and numerical [4], [5] results have been obtained at Reynolds numbers up to 100 which are well modeled by the correlation given in [2]. For intermediate shapes between discs and spheres, Masliyah and Epstein [6] performed numerical studies for Reynolds numbers up to 100, but no correlation was developed.

This work extends the efforts of previous contributions in providing an accurate model of the drag coefficient as a function of the aspect ratio of the ellipsoids, and in addition increases the range of Reynolds numbers over which the correlations can be applied. The drag response is numerically evaluated using an adaptive, *hp*-finite element method. Because this algorithm is higher-order accurate spatially and adapts the mesh based on solution requirements, we are able to obtain predictions of the drag to within 1%. This allows us to confidently evaluate previous models and, as needed, develop a more reliable one.

The paper begins with a formulation of the problem describing the relevant physical parameters governing our study. Next is a brief description of the numerical method and a validation of its accuracy. The current models used to predict drag are then summarized, and the remaining sections examine the results. In these sections, new correlations are developed for predicting the drag response of an ellipsoid as a function of Reynolds number and particle shape.

2. **Formulation**

The problem is that of axisymmetric fluid flow over an ellipsoidal particle. The fluid is assumed incompressible with constant density, ρ, and viscosity, μ. The shape of the particle is defined by its aspect ratio, E, which is the ratio of the length along the axis of symmetry to the maximum diameter normal to the axis. For $E < 1$, we have an oblate particle and for $E > 1$, we have a prolate particle. Since prolate particles tend to align themselves with their maximum cross section normal to the direction of the flow and thus do not remain axisymmetric, we will limit the study to oblate particles.

We study the drag force on the particle for a given aspect ratio and Reynolds number, $Re = \rho v_\infty d/\mu$, where v_∞ is the free-stream velocity and d is the cross-sectional diameter of the particle. Calculations are performed for $Re < 200$. Above $Re = 200$, it has been shown for spheres that the flow transitions to a non-axisymmetric solution [7]. The main goal is to obtain an accurate prediction of the drag on an ellipsoid as a function of the Reynolds number and aspect ratio. Simulations are performed in intervals of $\Delta E = 0.1$ from a disc ($E = 0$) to a sphere ($E = 1$) over the range of $0.1 < Re < 200$.

3. **Numerical Method**

A *hp*-finite element method is used to perform the numerical simulations [8]. For the calculations performed in this study we use a basis composed of quartic polynomials on each element ($p = 4$). Quartic polynomials are used because they allow rapid convergence to the exact drag value with increasing mesh resolution (5th order spatial accuracy). When examining the element meshes, note that the flow resolution is actually four times the element resolution because of the number of independent basis functions on each element.

The method uses an unstructured triangular mesh which is adapted based on the local accuracy of the solution [9]. The adaptation algorithm requires an input value of the maximum-allowable local truncation error in the total pressure, $p+1/2\rho(u^2+v^2)$, where p is the pressure and u, v is the flow velocity vector. This value was configured to give results for the drag which are accurate to within 1%. This was confirmed for flow over a sphere by varying the local truncation error input value until three significant figures of accuracy were obtained. Furthermore, in the extreme case of flow over an infinitely thin disc, low Reynolds number results are in good agreement with the analytic solution for Stokes flow [2] .

A rectangular domain is used in all the calculations. Figure 1 shows a typical element mesh which has been adapted to obtain the drag over a sphere at $Re = 200$. An inflow condition is enforced at the lower boundary of the mesh with (u, v) = (0,1) such that the flow is from bottom to top. At the downstream and right boundary, the total stress is set to zero. Along the centerline, a symmetry boundary condition is imposed, and on the particle a no slip boundary condition is imposed. The downstream boundary is from (0, 30) to (20, 30), and the inflow boundary is from (0, -20) to (20, -20) where the units are sphere diameters. It was shown in [8] that for a similar configuration the error associated with the far-field boundaries affects the drag by less than 1%.

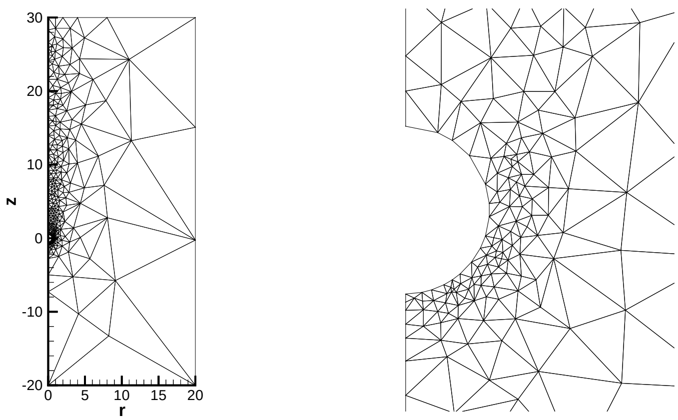

Figure 1: Typical element mesh with an insert of the region around the particle

4. Drag Models

The drag coefficient, C_D, is defined using the cross-sectional area normal to the direction of the flow such that:

$$C_D = \frac{D}{\frac{1}{2}\rho v_\infty^2 A} \quad (1)$$

where D is the drag force and A is the cross-sectional area. Previous numerical and experimental work provides us with many empirical equations for the drag on a sphere. For the Reynolds number range of interest, $0.1 < Re < 200$, Clift et al. [2] suggests the following correlations that are divided into two intervals:

$$C_{D_{Sphere}} = \frac{24}{Re}[1 + 0.1315 Re^{0.82 - 0.05 log_{10} Re}] \quad 0 < Re \leq 20$$

$$C_{D_{Sphere}} = \frac{24}{Re}[1 + 0.1935 Re^{0.6305}] \quad 20 \leq Re \leq 260 \quad (2)$$

Likewise for a disc, previous researchers have measured the drag response for steady flow parallel to the axis. Extensive experimental results at low and intermediate Reynolds numbers are well predicted [2] by:

$$C_{D_{Disc}} = \frac{64}{\pi Re}[1 + 10^{x}] \quad 0.01 < Re \leq 1.5$$

$$x = -0.883 + 0.906 log_{10} Re - 0.025 (log_{10} Re)^2 \tag{3}$$

$$C_{D_{Disc}} = \frac{64}{\pi Re}[1 + 0.138 Re^{0.792}] \quad 1.5 < Re \leq 133$$

It should be noted that there is no model validated for a disc for $Re > 133$.

To predict the dependence of drag on aspect ratio, several models have been proposed. In Stokes flow, there is an analytic solution given by:

$$\frac{C_{D_{Ellipse}}}{C_{D_{Sphere}}} = \frac{4}{3} \frac{1 - E^2}{[(1 - 2E^2) cos^{-1} E / \sqrt{1 - E^2}] + E} \tag{4}$$

where $C_{D_{Ellipse}}$ and $C_{D_{Sphere}}$ are for particles of the same equatorial diameter. In [2] it is has been suggested that this dependence of drag on aspect ratio for Stokes flow can be used to predict the behavior at higher Reynolds numbers.

Another possibility is to use a linear model, as presented in [10], to interpolate between the drag on a disc and a sphere:

$$C_{D_{Ellipse}} = E C_{D_{Sphere}} + (1 - E) C_{D_{Disc}} \tag{5}$$

Unlike the Stokes flow model, this model requires both the drag on a sphere and a disc.

5. Results

All of the models mentioned in the above section are rigorously analyzed over the entire range of Reynolds numbers. Results for spheres and discs, including oblate spheroids, are quantified here.

The drag coefficient on oblate particles are numerically evaluated in the range of $0.1 < Re < 200$. Simulations are performed for a disc ($E = 0$) and a sphere ($E = 1$) and in intervals of $\Delta E = 0.1$. Since the models for ellipsoids require the drag on a sphere and a disc, we begin by examining sphere and disc drag correlations. Equation 2 for a sphere is within 2% of our numerical results for $0.1 < Re < 200$. For the disc, equation 3 is within 2.5% of our numerical results for $0.1 < Re < 133$. However, the error begins to increase rapidly for $Re > 133$. Since our goal is to extend the range to $Re < 200$, a new model is developed for drag on a disc, which is shown by the following equation:

$$C_{D_{Disc}} = \frac{64}{\pi Re}[1 + 0.1241 Re^{0.8369}] \quad 0 < Re \leq 20$$

$$C_{D_{Disc}} = \frac{64}{\pi Re}[1 + 10^{x}] \quad 20 \leq Re < 200 \tag{6}$$

$$x = -1.1656 + 1.1885 log_{10} Re - 0.1223(log_{10} Re)^2$$

The new correlation is divided into two intervals similar to that of the sphere. Over the range $0.1 < Re < 200$, the numerical results for a disc are predicted to within 1%.

To determine the accuracy of the ellipsoid models discussed in Section 4, Figure 2 compares drag results from equations 4 and 5 and the numerical results for $E = 0.2$, 0.5 and 0.8. For the values of drag on a sphere and a disc, we use the correlations given by equations 2 and 6. In predicting the variation of drag on E, the Stokes solution performs well below $Re = 10$ but fails to predict the behavior at higher Re. The linear model is, by definition, as accurate as the disc and sphere correlations at the endpoints $E = 0$ and 1, but at intermediate values ($E = 0.5$) it deviates from the numerical results. At higher Re, it performs better than the Stokes result.

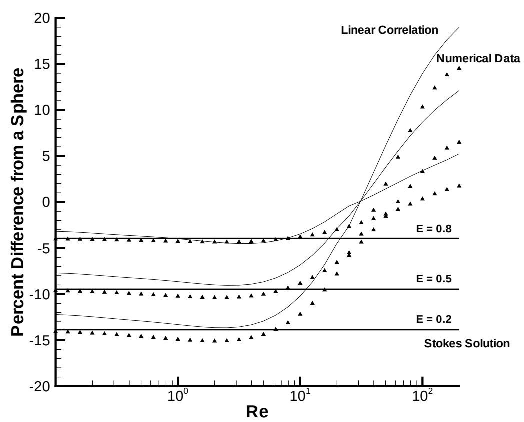

Figure 2: Linear Correlation - Percent Difference from a Sphere vs. Re

To show the dependence on aspect ratio, E, Figure 3 plots the above results as a function of E for $Re = 0.1$, 10, and 100. The same trend is observed as in Figure 2 where the Stokes solution performs well in the low Re limit. At higher Reynolds numbers however, it fails to capture the fact that the drag on a disc is actually greater than that of the sphere. The error in the linear model is proportional to the curvature in the numerical data.

To improve the accuracy of the linear model, a quadratic model is developed. Since the bulk of the error in the linear model occurs near $E = 0.5$, a correlation is developed for drag on an ellipsoid of $E = 0.5$. The following equation predicts the numerical data to within 1%:

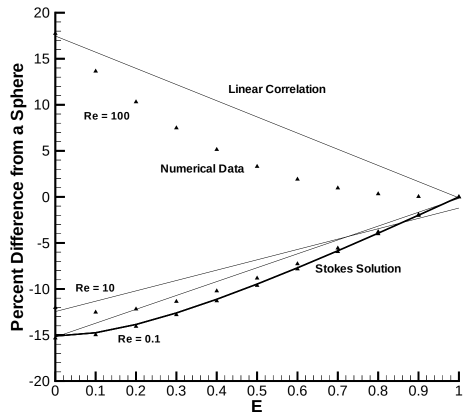

Figure 3: Linear Correlation - Percent Difference from a Sphere vs. E

$$\frac{C_{D_{0.5}}}{C_{D_{Sphere}}} = 0.9053[1 + 10^{-2.9570+1.2006log_{10}Re-0.0708(log_{10}Re)^2}] \quad 0 < Re \leq 20$$

$$\frac{C_{D_{0.5}}}{C_{D_{Sphere}}} = 0.9053[1 + 10^{-4.2784+2.9449log_{10}Re-0.6160(log_{10}Re)^2}] \quad 20 \leq Re < 200 \tag{7}$$

The leading term in these models is found by substituting $E = 0.5$ into the analytic solution for Stokes flow shown in equation 4. Using this correlation along with that of the sphere (equation 2) and the improved disc model (equation 6), a quadratic interpolation of the drag can be formed as a function of E. Equation 8 is constructed using a Lagrange interpolating polynomial with the coefficients as known values for $E = 0.0$, 0.5 and 1.0:

$$C_{D_{Ellipse}} = 2(E-1)(E-0.5)C_{D_{Disc}} - 4E(E-1)C_{D_{0.5}} + 2E(E-0.5)C_{D_{Sphere}} \tag{8}$$

To determine the accuracy of the quadratic model discussed above, Figure 4 compares drag results from the model in equation 8 and the numerical results. The quadratic fit accurately predicts the drag behavior over the entire range of parameters.

This is also confirmed by Figure 5, which plots the above results as a function of E for $Re =$ 0.1, 10, and 100. The numerical data proves to be well correlated to within an error of 1.5% with the quadratic fit.

6. **Conclusion**

The governing equations for two-dimensional axisymmetric flow of an incompressible fluid over an oblate particle have been solved numerically using a *hp*-finite element method. Values of drag were computed over a Reynolds number range from 0.1 to 200. The analytic solution

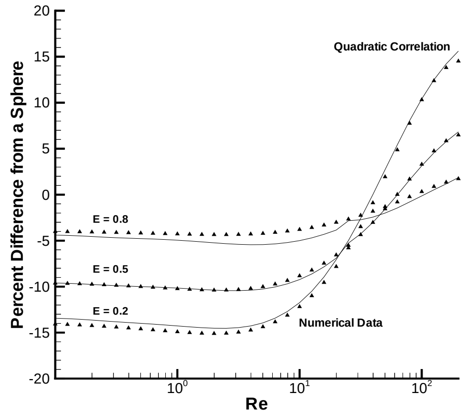

Figure 4: Quadratic Correlation - Percent Difference from a Sphere vs. Re

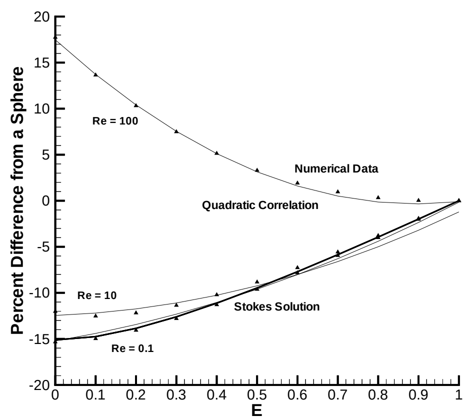

Figure 5: Quadratic Correlation - Percent Difference from a Sphere vs. E

to Stokes flow shows good agreement for $Re < 10$. A linear model between the disc and sphere drag gives a better approximation at higher Re, but leaves more to be desired for intermediate values of E. An attempt to merge these models, such that we obtain high accuracy in all limits, yielded a quadratic representation of the data as a function of E. This new model predicts the data to within 1.5% over the entire range of parameters.

REFERENCES

[1] J. Happel and H. Brenner. *Low Reynolds Number Hydrodynamics.* Prentice Hall, NJ, 1965.

[2] R. Clift, J. R. Grace, and M. E. Weber. *Bubbles, Drops, and Particles.* Academic Press, 1978.

[3] R. L. Pitter, H. R. Pruppacher, and A. E. Hamielec. *J. Atmos. Sci.*, 30:125–134, 1973.

[4] P. Michael. *Phys. Fluids*, 9(3):466–471, 1966.

[5] B. Munshi, R. Chhabra, and P. Ghoshdastidar. *Can. J. of Chem. Eng.*, 77:113–118, February 1999.

[6] J. H. Masliyah and N. Epstein. *J. Fluid Mech.*, 44:493–512, 1970.

[7] T. A. Johnson and V. C. Patel. *J. Fluid Mech.*, 378:19–70, 1999.

[8] B. T. Helenbrook. *Comp. Meth. Appl. Mech. Eng.*, 191:273–294, 2001.

[9] B. T. Helenbrook and T. J. Baker. In *Proceedings of the 2002 Joint ASME/European Fluids Engineering Division Summer Conference*, Montreal, Quebec, Canada, July 2002.

[10] L. P. Hsiang and G. M. Faeth. *Int. J. Multiphase Flow*, 18(5):635–652, 1992.